

Organic photovoltaics: The current challenges ^F

Cite as: J. Chem. Phys. **158**, 110901 (2023); <https://doi.org/10.1063/5.0139457>

Submitted: 20 December 2022 • Accepted: 13 February 2023 • Published Online: 15 March 2023

Published open access through an agreement with JISC Collections

 William Lowrie,  Robert J. E. Westbrook,  Junjun Guo, et al.

COLLECTIONS

 This paper was selected as Featured



View Online



Export Citation



CrossMark

ARTICLES YOU MAY BE INTERESTED IN

[Phase diagrams—Why they matter and how to predict them](#)

The Journal of Chemical Physics **158**, 030902 (2023); <https://doi.org/10.1063/5.0131028>

[Solving the Wigner equation for chemically relevant scenarios: Dynamics in 2D](#)

The Journal of Chemical Physics **158**, 114111 (2023); <https://doi.org/10.1063/5.0135540>

[Comparison of Matsubara dynamics with exact quantum dynamics for an oscillator coupled to a dissipative bath](#)

The Journal of Chemical Physics **158**, 114106 (2023); <https://doi.org/10.1063/5.0138250>



Time to get excited.
Lock-in Amplifiers – from DC to 8.5 GHz

[Find out more](#)



Organic photovoltaics: The current challenges

Cite as: *J. Chem. Phys.* **158**, 110901 (2023); doi: [10.1063/5.0139457](https://doi.org/10.1063/5.0139457)

Submitted: 20 December 2022 • Accepted: 13 February 2023 •

Published Online: 15 March 2023



View Online



Export Citation



CrossMark

William Lowrie,¹  Robert J. E. Westbrook,²  Junjun Guo,¹  Hristo Ivov Gonev,¹  Jose Marin-Beloqui,³ 
and Tracey M. Clarke^{1,a)} 

AFFILIATIONS

¹ Department of Chemistry, University College London, Christopher Ingold Building, London WC1H 0AJ, United Kingdom

² Department of Chemistry, University of Washington, Seattle, Washington 98195, USA

³ Departamento de Química Física, Universidad de Malaga, Campus Teatinos s/n, 29071 Málaga, Spain

^{a)} Author to whom correspondence should be addressed: tracey.clarke@ucl.ac.uk

ABSTRACT

Organic photovoltaics are remarkably close to reaching a landmark power conversion efficiency of 20%. Given the current urgent concerns regarding climate change, research into renewable energy solutions is crucially important. In this perspective article, we highlight several key aspects of organic photovoltaics, ranging from fundamental understanding to implementation, that need to be addressed to ensure the success of this promising technology. We cover the intriguing ability of some acceptors to undergo efficient charge photogeneration in the absence of an energetic driving force and the effects of the resulting state hybridization. We explore one of the primary loss mechanisms of organic photovoltaics—non-radiative voltage losses—and the influence of the energy gap law. Triplet states are becoming increasingly relevant owing to their presence in even the most efficient non-fullerene blends, and we assess their role as both a loss mechanism and a potential strategy to enhance efficiency. Finally, two ways in which the implementation of organic photovoltaics can be simplified are addressed. The standard bulk heterojunction architecture could be superseded by either single material photovoltaics or sequentially deposited heterojunctions, and the attributes of both are considered. While several important challenges still lie ahead for organic photovoltaics, their future is, indeed, bright.

© 2023 Author(s). All article content, except where otherwise noted, is licensed under a Creative Commons Attribution (CC BY) license (<http://creativecommons.org/licenses/by/4.0/>). <https://doi.org/10.1063/5.0139457>

INTRODUCTION

The performance of organic photovoltaic (OPV) devices has drastically improved over the last few decades, but with climate change at the forefront of the world's attention, the development of this sustainable energy solution is now more important than ever. Commercially available photovoltaics are traditionally fabricated from inorganic semiconductors such as silicon; however, “next-generation” materials such as perovskites and organics are rapidly gaining in feasibility. Although still lower in efficiency, OPV cells have considerable advantages: short energy payback times, the ability to be printed in high-throughput manufacturing processes, and high red–NIR absorptivity in very thin films. Combined, these characteristics could enable their incorporation into visibly transparent windows, significantly enhancing the commercial feasibility of building-integrated photovoltaics and providing another crucial tool in the arsenal to fight climate change.

After years of stagnant OPV device efficiencies, the OPV field is currently enjoying a renaissance, with power conversion

efficiencies now approaching 20%. This is due to the advent of non-fullerene electron acceptors (NFAs), which have largely replaced the more conventional fullerene (C₆₀) acceptors. Non-fullerenes offer multiple benefits over fullerenes, including substantially higher absorptivities and greater synthetic tuning for specific matching to a donor, with their typically planar structures often enabling improved electron mobilities. In 2017, Zhao *et al.* reported on the first OPV making use of a non-fullerene acceptor that exceeded the power conversion efficiencies of fullerene-based cells.¹ They made use of a fluorinated PBDB-T donor and a fluorinated non-fullerene ITIC [3,9-bis(2-methylene-(3-(1,1-dicyanomethylene)-indanone)-5,5,11,11-tetrakis(4-hexylphenyl)-dithieno[2,3-d:2',3'-d']-s-indaceno[1,2-b:5,6-b']dithiophene) acceptor (selected structures are shown in Fig. 1), achieving a power conversion efficiency (PCE) of 13%. Since then, NFA-based OPV devices have been steadily climbing in efficiency, recently reaching 19% in 2022.²

These recent advances in device efficiencies have spurred more research into the fundamental properties of these NFA materials, uncovering numerous intriguing results, a few of which will

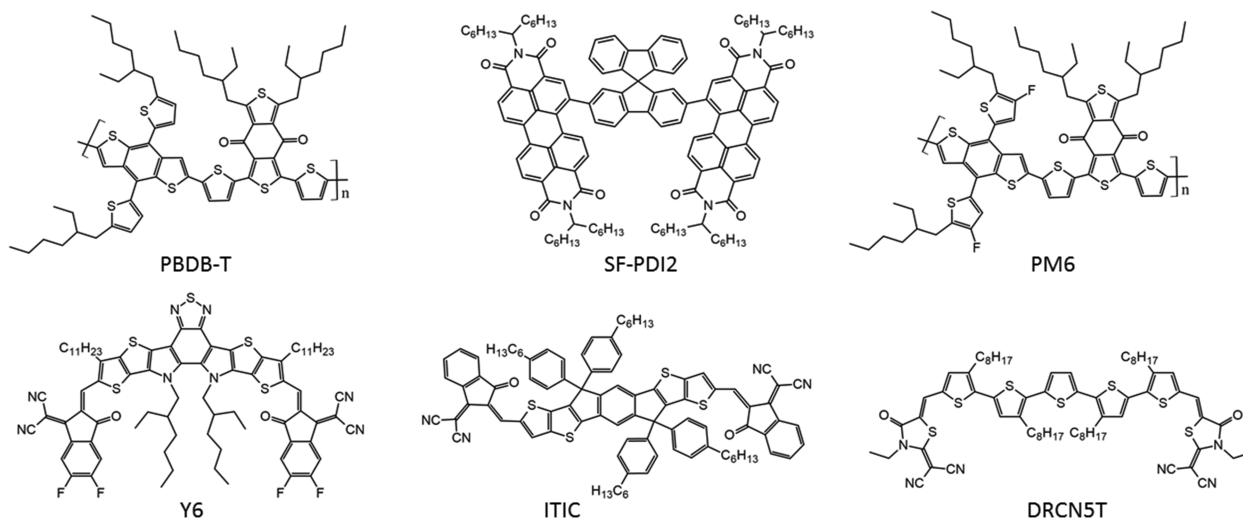


FIG. 1. Structures of selected small molecule donor and acceptors and polymers referred to in the text.

be discussed in this perspective article. This is not meant to be a comprehensive review, as new discoveries in recent years have inspired several excellent and detailed reviews.^{3–8} Instead, this perspective article will focus on selected key challenges—by no means an exhaustive list—that remain to first understand and then implement OPVs. We will cover topics that influence both fullerenes and NFAs, encompassing energy offsets and hybridization, non-radiative recombination, the effects of triplet states, and progress toward simpler device architectures.

ENERGY OFFSETS AND HYBRIDIZATION

Organic solar cells require both an electron donor and acceptor to separate excitons into the free charges that produce electricity. After the photoexcitation of a donor or acceptor molecule to form an exciton, the exciton must first diffuse to the donor/acceptor interface. There, the exciton can dissociate to form a charge transfer (CT) state via electron or hole transfer. Due to the typically low dielectric constants of organic materials, the exciton has a high binding energy. This energy barrier must be overcome for the exciton to separate into an electron and a hole and produce photocurrent. The magnitude of the Coulombic attraction between an electron and a hole can be calculated using Coulomb's law [Eq. (1)] and is significantly greater than the thermal energy at room temperature ($k_B T = 0.025$ eV),

$$V = \frac{e^2}{4\pi\epsilon_r\epsilon_0 r}, \quad (1)$$

where e is the charge of an electron, ϵ_r is the dielectric constant of the organic material in question, ϵ_0 is the vacuum permittivity, and r is the electron–hole separation.

The traditional viewpoint of OPV charge generation mechanisms requires a driving force—an “energy offset”—to overcome the exciton binding energy (Fig. 2). In a typical organic solar cell, the frontier energy levels of the donor and acceptor must have an

energetic offset that provides this driving force to split the exciton efficiently. The driving force then originates from the energetic difference between the singlet exciton (S_1 state) and CT state energies, ΔE_{S_1-CT} . Here, we define the concept of “energy offset” as the LUMO level offset when referring to electron transfer or the HOMO level offset when referring to hole transfer, although it should be pointed out that ΔE_{S_1-CT} is an equally valid definition. The CT state must then dissociate into free charges, forming the charge separated (CS) state. The magnitude of the driving force required for efficient charge photogeneration has been the source of significant research with numerous viewpoints offered. One school of thought, for example, is that excess driving force enables a vibrationally excited (“hot”) CT state that then provides an impetus for ballistic electron transport, enabling the CT state to overcome its own binding energy and form free charges.⁹ Lane *et al.* showed a link between excitation energy and photocarrier mobility, suggesting that “hot” excitons will form “hot” CT states at the interface.¹⁰ Additionally, a study by Tamura and Burghardt using the density functional theory (DFT) concluded that charge separation occurs via “hot” CT states.¹¹ They also noted that the excess vibrational energy was particularly beneficial to charge separation when the excess energy was near that of the exciton binding energy. It has also been suggested that it is the wave function delocalization of the hot CT state rather than the energy gradient that enables facile charge separation.^{12–14}

However, the importance of a hot CT state has faced disagreement from other groups. In one study, Vandewal *et al.* found that the internal quantum efficiency of selected polymer:fullerene systems remained high even if the CT state manifold was directly accessed.¹⁵ They attribute this observation to the ultrafast rate of vibrational relaxation of hot CT states, which outcompetes charge separation, thereby leading to charge photogeneration from relaxed CT states.

Some of the disagreement—but not all—arises from semantics and the definition of the term “CT state.” Here, we define it as the intermolecular donor/acceptor CT state intermediate formed during charge photogeneration, and it is distinct from a local singlet exciton.

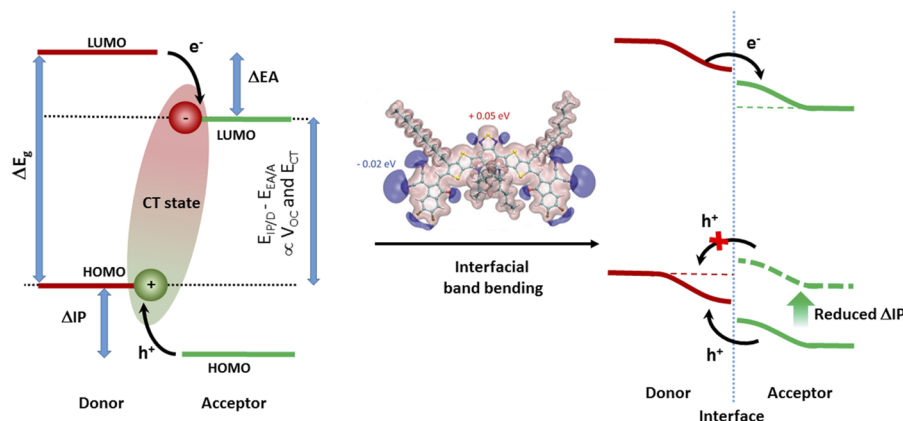


FIG. 2. Energy levels of the donor and acceptor in an organic solar cell, depicting the difference in HOMO levels (the change in ionization potential, ΔIP) and LUMO levels (the change in electron affinity, ΔEA), both without (left) and with (right) the interfacial band bending created by the quadrupole moments of NFAs. The calculated isosurfaces of the electrostatic potential of Y6 leading to its large quadrupole moment are shown [reproduced with permission from Perdigón-Toro *et al.*, *Adv. Mater.* **32**, e1906763 (2020). Copyright 2020 Wiley-VCH GmbH, Weinheim]. Also shown is the effect at negligible HOMO offsets (reduced ΔIP), where the band bending creates a barrier to exciton dissociation via hole transfer.

Altering the excitation wavelength to access different vibrational levels within the local singlet exciton manifold, for example, will not necessarily probe the presence or effects of hot CT states, particularly if vibrational relaxation within the singlet excitation manifold is very rapid.

To address the ambiguity in the role of “hot” states, Sosorev *et al.* considered a two-step charge generation model assuming the presence of “hot” CT states.¹⁶ An analysis using this model led them to propose two categories of OPVs: “CT state dissociation limited” and “CT state generation limited.” They suggest that charge generation in “CT state dissociation limited” systems is enhanced by “hot” CT states providing energy to overcome a significant charge separation barrier, while the latter possess a smaller barrier and are therefore limited by the rate of CT state formation.

The open-circuit voltage (V_{OC}) and short-circuit current (J_{SC}) of an OPV device are in delicate balance, with the optimization of one often being at the cost of the other. For example, increasing the interfacial energy offset between the donor and acceptor may increase the photocurrent but will simultaneously limit the V_{OC} . Therefore, a great deal of research is currently focused on minimizing the energetic offset at OPV heterojunctions. However, if the reduced energy offset is achieved by widening the bandgap of one component, this can also reduce the J_{SC} . How then do we achieve both high current and high voltage in an organic solar cell?

In 2015, Takimiya *et al.* demonstrated remarkably low voltage losses of ~ 0.52 eV in a polymer:fullerene blend with an ~ 0.1 eV LUMO offset between the donor and acceptor materials, showing that the small offset did not limit charge separation in this case.¹⁷ The following year, Liu *et al.*¹⁸ showed efficient charge generation in a polymer:NFA solar cell with a negligible energetic offset. Their blend exhibited a photoinduced electron transfer of 3 ps and a high electroluminescence quantum yield, enabling much higher solar cell efficiencies despite the observed minimal difference in singlet exciton and CT state energies. Since then, several more systems, including either fullerene or NFAs, have been observed to undergo

efficient charge photogeneration with a minimal energetic offset, sparking a flurry of research activity to uncover the fundamental reasons behind these observations.

A central issue in understanding the effects of minimal energy offsets lies in the method used to determine an accurate numeric value for the energy offset itself. No standardized method for determining ionization potential (IP) or electron affinity (EA) exists. This is exemplified by the wide range of PCBM LUMO level energies reported in the literature, which range from 3.7 to 4.3 eV.^{19–22} The results from current methods, including cyclic voltammetry and photoelectron spectroscopy, are typically only compared within the same method. Yet, even for cyclic voltammetry, differences arise from using peak potentials vs onsets, and even variations in the position of the natural hydrogen electrode relative to vacuum to provide the conversion factor between volts and electron volts.²³ Furthermore, EA and IP values can alter from the pristine material to the blend,²⁴ adding an additional element of complexity. Given the large uncertainties in EA and IP values, this creates an inherent difficulty in quantifying energy offsets, particularly in the minimal offset regime, where the singlet and CT emission spectra overlap.

A key aspect of NFAs is that they absorb light strongly, in stark contrast to traditional fullerenes. This opens up the probability of both the donor and acceptor contributing to charge photogeneration by hole transfer from the acceptor in addition to the standard electron transfer from the donor polymer. Zhong *et al.*²⁵ demonstrated that this hole transfer can occur on sub-picosecond timescales, even in the absence of an energetic offset. They used planar heterojunctions and dilute blends in addition to device-optimized blends to decouple charge transfer and exciton diffusion, enabling intrinsic charge transfer rates to be determined. Intriguingly, while the hole transfer rate was, indeed, correlated with a driving force, all rates were sub-picoseconds, even when the driving force approached zero. Zhong *et al.* attributed this to the low reorganization energies associated with the hole transfer process.

Indeed, it has been shown that the electron transfer channel in non-fullerene blends can be inoperable due to the ultrafast singlet energy transfer from the polymer to the NFA.²⁶ As such, the LUMO level offset may be less relevant in these cases. However, Karuthedath *et al.* also suggest a minimum ionization potential offset of 0.5 eV to ensure an efficient charge transfer. They relate this to band-bending at the donor/acceptor interface (Fig. 2), which essentially increases the ionization energy of the donor and decreases the electron affinity of the acceptor, effectively increasing the CT state energy. This band-bending inhibits exciton dissociation into CT states at low ionization energy offsets by creating a negative driving force for exciton dissociation under these conditions. Natsuda *et al.* suggested that energy and charge transfer are in competition in contemporary OPV blends, with smaller domains favoring the latter.²⁷

The band bending observed in non-fullerene blends is caused by the electrostatic interaction of the charges with the large quadrupole moments of the NFA molecules. Quadrupole moments are large in NFA materials because their typical A–D'–A'–D'–A molecular architecture induces an alternating charge density “checkerboard pattern,” which is enhanced due to the aggregation properties of NFAs.²⁸ While Karuthedath *et al.*²⁶ show that the band-bending is detrimental to the conversion of excitons to CT states, they also highlighted that it is favorable for the CT state dissociation into free charges. This was beautifully demonstrated by Perdigón–Toro *et al.* one year earlier for the high-performing PM6:Y6,²⁹ showing that its barrierless CT state dissociation was possible due to Y6's large quadrupole moment (Fig. 2) and the resulting electrostatic interfacial field that compensates for the Coulomb dissociation barrier.

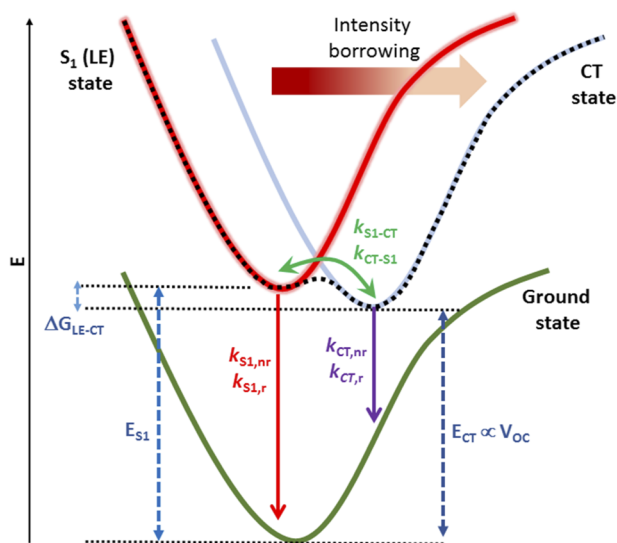


FIG. 3. Potential energy surfaces illustrating the hybridization between the bright LE/S₁ and dark CT states at small energy offsets (small ΔG_{LE-CT}), enabling an increase in the oscillator strength of the CT state via intensity borrowing. Pertinent rate constants are shown, including the radiative (r) and nonradiative (nr) decays back to the ground state and the facile interconversion between LE and CT states (k_{S_1-CT} and k_{CT-S_1}) enabled by their enhanced coupling.

Minimizing the energetic offsets has a natural consequence that the CT state is energetically very close to the singlet state [local exciton (LE)]. Importantly, this can lead to a hybridization between the two states (Fig. 3).³⁰ One of the most important ramifications of this is that nonradiative voltage losses can be suppressed due to the resulting increase in the CT state luminescence,³¹ and this will be discussed in the section titled “NON-RADIATIVE RECOMBINATION AND THE ENERGY GAP LAW.” It has also been suggested by Hinrichsen *et al.*³² that this hybridization allows an equilibrium to form between singlet, CT, and CS states and that the dissociation of interfacial charge-transfer states is thermally activated rather than barrierless. In this case, it was suggested that the long lifetime of the disorder-free CT state enables no energetic offset requirement.

In a similar vein, Classen *et al.*³³ suggested that the key to achieving these high organic solar cell efficiencies at minimal energy offsets is a long exciton lifetime. The minimal energy offset inhibits the rate of exciton splitting (electron or hole transfer) at the donor/acceptor interface, and, therefore, a long exciton lifetime enables this slow exciton splitting to take place. For blends with Y6, one of the most efficient non-fullerene acceptors currently known, the exciton splitting efficiency is almost unity even at minimal energy offsets. The authors relate this to Y6's exceptionally and unusually long exciton lifetime of 1 ns. Classen's experimental findings are corroborated by including hybridization via a two-state model with local excitons in equilibrium with CT states. The researchers show that the exciton splitting efficiency is dictated by both the energetic offset and, crucially, the exciton lifetime.

However, an important point to note is that the singlet exciton/CT state hybridization and equilibria observed by multiple groups—and invoked to rationalize high-performing NFA systems—are not actually exclusive to NFAs. If a fullerene is matched with a very low bandgap polymer (thereby also yielding a negligible energy offset), the exciton and CT states will also hybridize and form an equilibrium. This minimizes non-radiative voltage losses in much the same way as non-fullerene acceptors can.³⁴ Despite this, such low offset fullerene devices still show substantially smaller power conversion efficiencies compared to recent low offset NFA systems. An important future step, then, is to decouple the magnitude of the energy offset from the identity of the acceptor to truly understand what makes NFAs so special. It appears that the large quadrupoles present for NFAs play a crucial role in this, but the opposing nature of the consequent band-bending—promoting CT state dissociation but inhibiting exciton dissociation at small energetic offsets—requires further investigation and new strategies to address this.

NON-RADIATIVE RECOMBINATION AND THE ENERGY GAP LAW

To enable organic photovoltaics to be competitive on the world stage, one of the most critical factors still to be solved is non-radiative decay back to the ground state. Within the context of OPVs, non-radiative decay usually refers to the relaxation of the interfacial donor/acceptor charge transfer state back to the ground state without photon emission, thereby losing the potential energy as heat. Even with the introduction of highly efficient non-fullerene acceptors pushing efficiencies close to 20%, non-radiative decay remains a major loss mechanism.

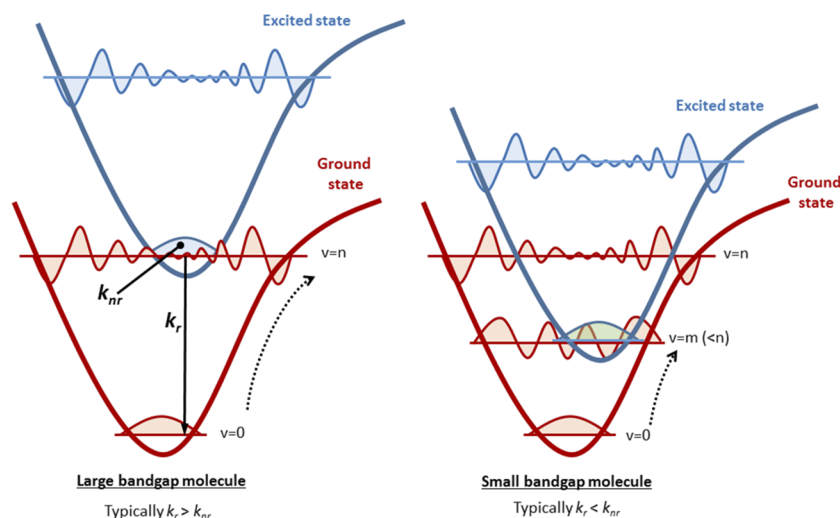


FIG. 4. Potential energy curve representation of non-radiative decay (k_{nr}) from an excited state to the ground state compared to radiative decay (k_r). The value of the rate coefficient k_{nr} is directly proportional to the wave function overlap of the two isoenergetic vibrational states. As the bandgap decreases, the vibrational wave function overlap increases (for a given ΔQ), thereby giving rise to the energy gap law.

To maximize light absorption across the solar spectrum, optical bandgaps are being pushed further into the near-infrared (NIR) and most NFAs absorb strongly in this region. Indeed, Y6, one of the highest performing NFAs so far, has an absorption maximum of around 800 nm. However, as the bandgap and thus the singlet exciton energy decrease, this typically increases the efficiency of non-radiative internal conversion (illustrated in Fig. 4). In general, the non-radiative decay involved in the deactivation of an excited state is typically internal conversion followed by vibrational relaxation. The internal conversion step involves a horizontal transition between two isoenergetic vibrational levels of the excited state and the ground state, the rate of which depends largely on the vibrational wave function overlap. This, therefore, gives rise to the energy gap law: within the weak coupling limit, as the energetic spacing between two electronic states decreases, the efficiency of internal conversion between them is exponentially increased.³⁵ Non-radiative relaxation can, therefore, become very fast in low bandgap materials, which typically precludes long exciton lifetimes and high photoluminescence yields.

Collado-Fregoso *et al.* demonstrated the presence of the energy gap law in polymer:fullerene blends using transient absorption spectroscopy. They investigated the effect of changing the CT state energy, thus altering ΔE_{S_1-CT} .³⁶ They found that, indeed, non-radiative geminate recombination from the CT state obeys the energy-gap law. Consequently, lowering the CT state energy enhances non-radiative geminate recombination, which the authors suggested is a result of increased vibronic coupling from the CT state to the ground state.

Non-radiative decay limits the efficiency of OPV devices by reducing the attainable V_{OC} . The V_{OC} of an OPV device, one of the primary parameters controlling device efficiency, is dictated by the non-radiative voltage losses subtracted from the radiative open-circuit voltage: $V_{OC} = V_{OC,rad} - V_{OC,nr}$. In turn, $V_{OC,nr}$ is dictated primarily by $\ln[k_r/(k_r + k_{nr})]$, where k_r and k_{nr} are the radiative and non-radiative decay rate coefficients, respectively. A zero k_{nr} leads to a zero $V_{OC,nr}$. For NIR-absorbing materials, therefore, the ultimate goal is to maximize k_r at the expense of k_{nr} , producing low

bandgap materials with long excited state lifetimes and high photoluminescence (PL) quantum yields. However, there is an inherent dichotomy between this ideal and the energy gap law that needs to be addressed, first by tackling the fundamental understanding of non-radiative decay in complex organic photovoltaic blends, which is still very much in progress.

The V_{OC} of an OPV device is intrinsically related to the energy gap between the HOMO of the donor and the LUMO of the acceptor and is thus closely connected to the energy of the CT state. One of the main impacts of minimal energy offset systems, therefore, is to maximize the achievable V_{OC} of a device. As mentioned in the section titled “ENERGY OFFSETS AND HYBRIDIZATION,” this has an additional effect of also reducing the energetic separation between the local singlet exciton state and the charge transfer state, enabling the two states to couple together (hybridization). It has been shown for both fullerene and NFA blends that this hybridization allows intensity borrowing: the typically dark CT state gains oscillator strength by coupling with the bright singlet exciton. Eisner *et al.*³¹ demonstrated this using a variety of both fullerene and non-fullerene blends with both experimental and simulation methods with a three-state model, showing a trend of lower non-radiative voltage loss as ΔE_{S_1-CT} is reduced. The lower non-radiative voltage losses arise from the enhanced oscillator strength of the CT to ground transition when the electronic coupling between the S_1 and CT states is strong. Notably, it is the lower bandgap material that should have a high $S_1 \rightarrow S_0$ oscillator strength: in NFA blends, this is typically the NFA rather than the polymer.

The importance of high photoluminescence and electroluminescence quantum yields to maximize V_{OC} was also reinforced by the design rules reported by Qian *et al.*³⁰ Furthermore, as ΔE_{S_1-CT} decreases, the reverse transition from the CT state back to the singlet state becomes more viable, thus enabling an additional radiative relaxation pathway and providing another avenue for the reduction in non-radiative decay losses. Indeed, Chen *et al.*³⁷ demonstrated that when ΔE_{S_1-CT} is small and hybridization is in play, the energy gap law is no longer adhered to due to the additional coupling effects of the bright local exciton. This conclusion further verifies that the

selection of donor and acceptor materials with high photoluminescence yields promotes high power conversion efficiencies. For example, it has been shown that relatively low non-radiative voltage losses of 0.15 eV are achievable in an NFA-based OPV device consisting of high photoluminescence yield materials.³⁸ However, Liu *et al.* noted that hybridization does not always lead to improved CT state photoluminescence and reduced voltage loss.³⁹ They showed that hybridization in one blend led to *faster* non-radiative recombination than predicted by the Marcus–Levich–Jortner model, making the case for consideration of both the radiative (k_r) and non-radiative (k_{nr}) rate coefficients of the neat components rather than just their photoluminescence quantum yields.

Interestingly, the recent computational and spectroscopic work by Azzouzi *et al.*⁴⁰ reports that reducing ΔE_{S_1-CT} in NFA blends decreases the rate coefficients of both singlet exciton and CT state dissociation, alongside an increase in free charge carrier recombination back to CT states. Furthermore, they note that a deeper donor ionization potential not only decreases ΔE_{S_1-CT} but also reduces the free energy offset between the CT state and the free charge carriers. These intriguing results provide a broader context for the effects of marginal offset systems, showcasing the trade-off between maximizing V_{OC} and maintaining reasonable J_{SC} and fill factor by demonstrating that the poorer performance in some low-offset systems can be caused by accelerated recombination of charges back to the CT state.

TRIPLETS

Triplet states commonly form during the operation of OPV cells.⁴¹ There are three main mechanisms by which donor or acceptor triplet states form in an organic solar cell, depicted in Fig. 5: intersystem crossing (ISC), back electron transfer from a spin-mixing charge transfer (CT) state,⁴² and bimolecular recombination of free carriers.⁴³ The latter two mechanisms, therefore, both proceed via a CT state and are dependent on the energetics of the system, kinetic competition, spin statistics, and the nature of the spin-mixing. The rate of ISC is controlled by the magnitude of the spin–orbit coupling and the energy gap between the singlet and triplet states involved, ΔE_{ST} . The spin–orbit coupling depends on either the presence of heavy atoms and/or changes in orbital angular momentum, whereas ΔE_{ST} depends on the exchange energy.

Interest in triplet states has been mounting owing to their recently discovered prevalence in highly efficient non-fullerene acceptor OPV blends.⁴⁴ Considering that triplet formation is traditionally seen as a loss mechanism in OPVs, this is a very surprising result. Since the T_1 state is often one of the lowest energy states of the system, for example, its formation and subsequent relaxation back to the ground state entail a non-radiative voltage loss. Gillett *et al.*⁴⁴ used a combination of transient absorption spectroscopy and electron paramagnetic resonance spectroscopy to show that a series of NFA-based OPV blends typically exhibited non-geminate NFA triplet formation in preference to geminate triplet formation, including the high-efficiency blend PM6:Y6. It was also noted that in the few blends without evidence of triplet formation via charges, high quantum yields of ISC were observed instead. Indeed, it is estimated that for certain blends, 90% of charge recombination occurred via the NFA triplet and this had a negative impact on the V_{OC} . However, the authors noted that hybridization between CT and local

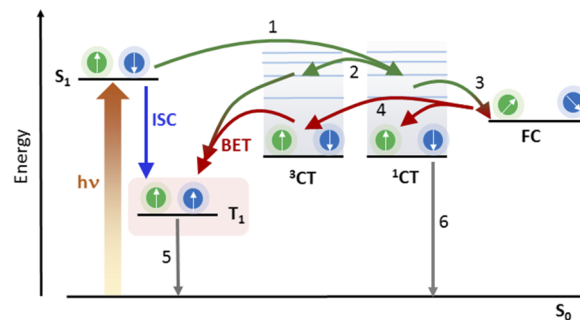


FIG. 5. Formation pathways for triplet states in organic solar cells. In intersystem crossing (ISC, blue), optical excitation to the singlet manifold (such as the S_1 state) on either the donor or acceptor is directly followed by relaxation to the triplet manifold (represented here for simplicity as only the T_1 state). Geminate triplet formation (green): the initial excitation is followed by exciton dissociation (1), resulting in a spin-mixing (2) CT state; back electron transfer (BET) from the 3CT state to the triplet manifold (T_1) then occurs rather than CT state dissociation into free charges (3, FC). In the non-geminate triplet formation pathway (red), the free charges recombine to reform the CT state (4), from which back electron transfer to the T_1 state on the donor or acceptor (depending on which has the lowest energy T_1 state) occurs.

excitons could destabilize the 3CT state at close donor–acceptor separations such that the back charge transfer to create the NFA triplet is suppressed.

Triplet formation is prevalent in polymer:fullerene blends as well. The generation of triplets rather than charge carriers necessitates that the polymer or fullerene triplet is lower in energy than the charge separated state. This is particularly likely for polymers with high ionization potentials (deep HOMO), as the high IP increases the energy of the CS state above either triplet, as has been reported for both polythiophene and polyfluorene systems.^{45,46} In 2015, Dimitrov *et al.*⁴³ reported one of the first demonstrations of a spin-mixing CT state that underwent geminate recombination to form triplet states. Importantly, they linked this to consequently lower free charge carrier yields and, thus, a lower device performance. More recently, Privitera *et al.*⁴⁷ suggest this geminate triplet formation to be a general phenomenon for fullerene-based blends.

Triplet formation can also depend on the morphology of the active layer. Rao *et al.*^{48,49} have shown that ordered fullerene domains enable wave function delocalization of the CT state. The greater effective separation of hole and electron promotes CT state separation over the competing process of back electron transfer to create triplets. In polymer:NFA blend systems, the triplet formation is also influenced by morphology. Gillett *et al.* have shown, for example, that the relative energies of the 1CT and 3CT states depend on the donor/acceptor spatial separation, where the 3CT state is destabilized and the 1CT stabilized at short distances due to hybridization between the CT and local excitons in PTB7-Th:IEICO-2F.⁴⁴ As such, 3CT states will favor interfacial sites where donor–acceptor spatial separations are larger. Since the donor–acceptor electronic coupling—and, hence, the back electron transfer rate—decreases with increasing spatial separation, this consequently reduces non-geminate triplet formation.

Fluorination has also been shown with both polymers⁵⁰ and acceptors⁵¹ to be an effective way to suppress triplet formation.

Wang *et al.* showed that the triplet formation via bimolecular recombination of charges was reduced upon fluorination of an IDIC-based NFA, resulting in an increased charge carrier lifetime and improved device performance.⁵¹ The authors attribute this to a modified energetic landscape, where fluorination causes an interfacial mixed $^3\text{CT}/^3\text{LE}$ state that is lower in energy than the T_1 state in the bulk NFA, thereby suppressing triplet generation via the non-geminate recombination pathway. It should be noted that fluorination can also alter other aspects such as morphology and charge carrier mobility. For example, Chen *et al.*⁵⁰ showed that non-geminate triplet formation was slower in the PM6:IXIC-4Cl blend compared to the PBDB-T:IXIC-4Cl blend, noting that PM6 contains fluorine atoms while its analog PBDB-T does not. The former blend shows a better device performance. Chen *et al.* ascribe their observation to the better π - π stacking and charge carrier mobility in the PM6:IXIC-4Cl film, which facilitate CT state delocalization and, thus, dissociation into free charge carriers.

An additional triplet pathway that can have a large negative influence on the OPV device performance is triplet-charge annihilation (TCA).^{49,52} It has not been frequently considered in the OPV literature, and its precise mechanism is poorly understood because TCA is typically inferred rather than directly observed. Our group recently reported a small molecule:fullerene system in which TCA was clearly demonstrated.⁵³ DRCN5T:fullerene blends—among the fullerene-based OPVs of highest efficiencies—showed a pronounced DRCN5T triplet formation. The TCA was demonstrated in both DRCN5T:fullerene and DRCN5T:NFA blends using microsecond-TAS, where the presence of triplet-quenching oxygen substantially enhanced the charge carrier population and lifetime. Although DRCN5T, with its high oxygen stability, offers an excellent opportunity to showcase TCA, it is reasonable to presume that this mechanism is prevalent in other blends, particularly in cases where charge densities are high.

Indeed, illuminated organic conjugated materials are well known to produce singlet oxygen ($^1\text{O}_2$) via Dexter energy transfer between the triplet and ambient $^3\text{O}_2$. This photochemistry is broadly exploited in the field of photodynamic therapy, where reactive $^1\text{O}_2$ species can be used to attack cancerous cells.⁵⁴ Despite this, remarkably few studies have focused on the role of $^1\text{O}_2$ in the degradation of OPV cells. Soon *et al.* reported that polymer films with a shorter triplet lifetime were generally more stable.^{55,56} They proposed that in these cases, the formation of $^1\text{O}_2$ was outcompeted by the thermal relaxation of the triplet state. However, the significance of this degradation pathway for working OPVs is debated, given that the concentration of O_2 in devices is typically low.

Research on the link between triplet states and stability is now largely focused on the intrinsic photo-instabilities in the bulk heterojunction (BHJ) itself, which cannot be mitigated by better encapsulation barriers. It is well known that triplet states in fullerene acceptors can mediate the dimerization of C_{60} via a $[2 + 2]$ cycloaddition.⁵⁷⁻⁶¹ Distler *et al.* proposed that this dimerization degrades performance by reducing the fullerene mobility.⁵⁹ Furthermore, Che *et al.* showed that triplet states can also catalyze degradative reactions in donor:NFA systems.⁶² Using IT-4F as an example, they showed that the six-electron photoisomerization between the dicyanomethylene unit and the thiophene ring was mediated by the acceptor triplet state. Recently, Luke *et al.* conducted a study to investigate the improved stability of ITIC-2F as

compared to ITIC and ITIC-DM. The authors proposed that the higher crystallinity of ITIC-2F compared to other IT-core derivatives reduces the likelihood of triplet formation, which, in turn, minimizes the possibility of photoisomerization.⁶³

Although traditionally seen as a loss mechanism, the unique properties of triplets are increasingly being manipulated to enhance device efficiencies through strategies such as singlet fission⁶⁴⁻⁶⁶ and up-conversion.^{67,68} Indeed, a number of groups have reported an enhancement in device efficiency with a higher triplet population,¹⁹⁻²¹ and some solar cells operate via the formation of triplets with a negligible direct formation of polarons.²²⁻²⁶ Despite the relatively low efficiency of these triplet solar cells, the point is clear: it is possible to extract energy from triplet states in a solar cell. Importantly, Laquai *et al.* showed that triplets could create polarons through triplet-triplet annihilation (TTA), enhancing the maximum theoretical efficiency.²⁷ New high energy singlets were created via TTA, where these singlet excitons had enough energy to undergo delayed charge separation on the nanosecond timescale.

There are a number of potential strategies for utilizing triplets in OPVs. The ΔE_{ST} in conjugated polymers is typically large, on the order of 0.7 eV.⁴¹ However, reducing this exchange energy has the potential advantage of allowing triplet recycling via reverse intersystem crossing (RISC). Reducing ΔE_{ST} is also necessary for thermally activated delayed fluorescence (TADF), a key strategy for enhancing organic light emitting diode (OLED) efficiencies. As such, the same orbital decoupling strategies employed in the TADF-OLED field could also be applicable for OPVs.

One of the key reasons that the influence of triplet states in OPVs is arguably less well understood than that of singlet excitons and charge carriers is because triplets are an intermediate species. Neither directly photogenerated nor extracted from a device, triplet parameters such as their absorption cross-section, actual populations, and quantum yields of creation/decay are often difficult to measure accurately. We took an important step in this regard recently by using triplet sensitization to measure the molar extinction coefficients of several key NFA triplets,⁶⁹ which should allow more facile analysis of triplets in NFA-based OPV blends in the future.

However, it is critical to quantify the effects triplets have on device performance. In this context, one of the most promising techniques is transient electrically detected magnetic resonance,⁷⁰ which can be performed on complete OPV devices. This technique, when combined with standard transient electron paramagnetic resonance, enables crucial links to be made between triplet formation/decay and the photocurrent produced by the device.

BEYOND BULK HETEROJUNCTIONS: SINGLE-MATERIAL AND SEQUENTIAL DEPOSITION DEVICES

One of the great paradigm shifts in the OPV field was the introduction of the BHJ architecture, which superseded the bilayer geometry. The BHJ architecture greatly increases the donor/acceptor interfacial area and, therefore, significantly improves exciton dissociation and charge generation. However, BHJs suffer from a major disadvantage in that the enhanced donor/acceptor interfacial area also considerably increases the probability of charge recombination. Despite this, BHJ architectures offer much better efficiencies

than the original strictly planar architectures. BHJs have been able to attain 19% efficiencies, while these bilayer architectures have achieved 5%.^{71–73}

However, the advent of new materials, particularly NFAs with their high mobilities and longer exciton diffusion lengths (20–50 nm),^{33,74} is promoting a resurgence in the bilayer concept. These have been called several names in the literature: planar-mixed heterojunctions, pseudo-bilayers, or planar heterojunctions. Such structures are typically achieved by sequential deposition (SD) of the donor and acceptor layers from solution via blade-coating or spin-coating, utilizing solvent orthogonality to form a bilayer with a highly textured interface (Fig. 6). The extent to which the two layers mix—and, thus, the donor/acceptor interfacial area—depends on factors such as solvent and donor/acceptor miscibility. The SD structure thus has an inherently reduced donor/acceptor interfacial area compared to a BHJ, often enabling an efficient exciton dissociation and charge extraction while also inhibiting charge recombination.^{75–78} Another advantage of planar geometries is the greater reproducibility because of a reduced dependence on microstructure and nanomorphology than BHJs. It is now possible to obtain high efficiency SD solar cells,^{79,80} with efficiencies of over 19% reported.^{81,82} In some cases, these SD efficiencies are on the same order as or even larger than their BHJ counterparts.^{83–88}

A major point of differentiation between SD devices and BHJs is that the SD strategy allows the processing and optimization of each individual layer. For instance, Dong *et al.* obtained optimum efficiency with donor and acceptor thicknesses of 90 and 30 nm for the

donor and the acceptor materials, respectively.⁸⁹ This fine control of device fabrication would not be possible with a BHJ architecture. This control of the individual layers has also enabled efficient SD devices with thick layers,^{90,91} an important requirement for OPV commercialization feasibility. Cai *et al.*, for example, used blade-coatings of thick sequential layers to obtain 16.9% efficiencies with a 300 nm thick active layer.⁹² This result was of particular interest because even thicker devices (500 nm) almost maintained that optimum efficiency (15.7%).

In line with this, it is possible to tune the molecular orientation in a planar heterojunction donor/acceptor interface.⁹³ The relative orientation at the donor/acceptor interface has been shown in the literature to be an important factor dictating the efficiency of key photophysical pathways.^{77,94,95} One of these pathways is the long-range energy transfer by Forster resonance, which can be enhanced in layer-based geometries. Park *et al.* distinguished energy transfer from charge transfer by incorporating an insulating layer between the donor and acceptor layers⁹⁶ and demonstrated that layer geometries facilitate considerably longer-range energy transfer than between isolated molecules or small domains. Energy transfer is known to be an important process in OPV blends and materials.^{26,97,98}

A remarkable point is that, in many cases, SD devices show better stabilities than their BHJ counterparts.^{84,85,87,89,90,93,99} For example, it is possible to adjust the layer ordering such that the more stable component receives the most light through the transparent electrode. Another origin for this larger stability is the intrinsically separated and purer phases of SD devices in comparison with BHJs.

Both BHJ and SD organic photovoltaic devices require two separate components blended together to form the active layer: the electron donor and acceptor. To achieve an efficient photovoltaic performance in organic materials requires both components to overcome the binding energy of the initial photogenerated exciton to create free charges. This is the case even for the highest efficiency OPV devices, which incorporate novel non-fullerene acceptors.^{100,101} Although efficient charge photogeneration can be achieved using this two-component configuration, it is accompanied by a host of other issues: energy losses,³⁴ morphology variations,¹⁰² miscibility,¹⁰³ stability,¹⁰⁴ and added fabrication complexity. It is, therefore, desirable to target OPVs with a single-material active layer.¹⁰⁵ However, organic small molecules and polymers on their own do not possess the high levels of charge photogeneration¹⁰⁶ or long charge carrier lifetimes required.¹⁰⁷ Indeed, while many pristine organic materials can generate charge carriers, these typically recombine on ultrafast timescales due to their inability to escape their mutual Coulombic attraction. Furthermore, many pristine conjugated polymers exhibit solely triplet formation.^{108,109}

The possibility of single-material OPVs has been examined in recent years with research into charge photogeneration in pristine, polycrystalline α -sexithiophene.¹¹⁰ Grain boundaries between crystalline domains possessing different molecular orientations generate the required interfacial energy offset for efficient exciton dissociation into free charges. Remarkably, an EQE of 44% and a V_{OC} of 1.61 V were achieved, highlighting the potential of single-material OPVs. A follow-up work¹¹¹ showed that while the exciton dissociation probability at a grain boundary was low (0.5%), the extraordinarily long exciton diffusion length of ~ 45 nm was able to compensate for this.

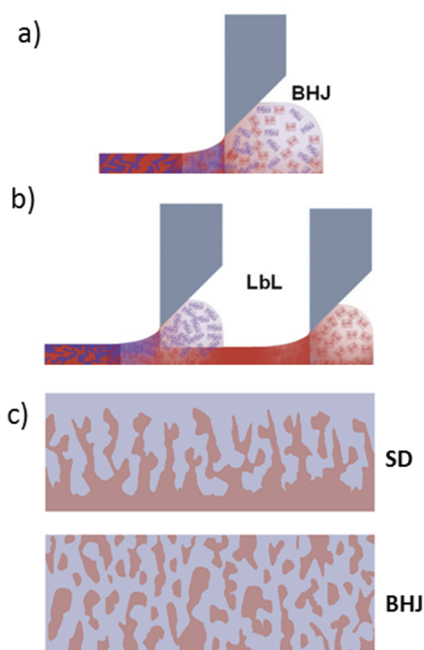


FIG. 6. An illustration of the differences between a coating of a BHJ (a) and a sequentially deposited (SD) device (b) via blade-coating; a representation of the morphologies formed in each case (c). Figures (a) and (b) are reproduced with permission from Sun *et al.*, *Energy Environ. Sci.* **12**, 3118 (2019). Copyright 2019 Royal Society of Chemistry.

Intrinsic charge photogeneration in the high-efficiency non-fullerene acceptor Y6 has also been observed.¹⁰⁷ High populations of charge carriers were observed at very early times, attributed to an intermolecular polarization pattern that promotes exciton dissociation. However, these charge carriers decayed back to the ground state rapidly, leading to poor-performing OPV devices. The desirable properties of Y6 as an electron acceptor have also led it to be incorporated into intramolecular donor/acceptor block copolymer structures for single material OPVs, but again, high levels of charge carrier recombination were reported.^{112,113}

Rather than a block copolymer strategy to incorporate both the donor and acceptor components, double-cable polymers have also been trialed for single-material OPVs. Typically, these materials have a polymer donor backbone with acceptor moieties as side chains that are required to stack together to create the necessary electron channels. One of the most successful was reported by Jiang *et al.*, who achieved a remarkable 8.4% OPV device efficiency.¹¹⁴ This was possible due to the fine-tuning of the miscibility by altering the position of Cl atoms such that exciton diffusion and dissociation were promoted.

Recently, we reported a novel conjugated polymer with a donor/orthogonal acceptor motif. The orthogonal acceptor spatially isolated the LUMO from the HOMO, allowing for intramolecular CT states to form. These CT states were able to dissociate into free charges in both the pristine solution and the film. The charge carriers possessed remarkably and unusually long millisecond lifetimes due to the stabilization imparted by the spatial separation of the polymer's donor and orthogonal acceptor motifs. Although this strategy mitigated the fast recombination observed in other pristine materials, another issue arose: the donor/orthogonal acceptor polymer was also able to efficiently produce triplet states on ultrafast timescales. While evidence existed that the triplet and charge carrier generation were linked, the excessive triplet formation still limited charge photogeneration yields.

Single-material OPVs remain an extremely worthwhile goal, but there remain significant questions to be answered. Charge carriers need to be produced with high yields and long lifetimes. Furthermore, these carriers must be able to be extracted in a device. Finally, in order to be commercially viable, the synthesis must be scalable in an industrial setting, which may place limitations on the complex donor-acceptor copolymer design.

CONCLUDING REMARKS

Extensive research has been conducted over the last few decades with the aim of increasing the power conversion efficiencies of OPV devices. In particular, a thorough understanding of the photophysics and device physics involved will be required for future organic devices to match the efficiencies displayed by the current state-of-the-art inorganic cells. After the relatively recent emergence of high efficiency NFA blends, it has become apparent that NFAs possess several key characteristics that have led to significant efficiency increases in the last few years: high absorption coefficients, strong packing motifs, synthetic tunability, and the ability to generate charges with low energy offsets. The trade-off between V_{OC} and J_{SC} that once hindered the performance of fullerene devices can be overcome. Newfound importance is now placed on long exciton lifetimes, favorable interfacial electrostatics, and wave function

delocalization at the interface to reduce the effective exciton binding energy *in lieu* of a significant energy offset to provide a driving force. These properties have been demonstrated in non-fullerene acceptors such as Y6, which has been successfully used in several state-of-the-art organic devices reaching efficiencies of 19%. However, there are still several aspects of OPV materials and devices that need to be tackled, including the role of triplet states, the current dependence on BHJ architectures, and non-radiative voltage losses. It is likely that further improvement in the OPV device performance and enhancement in their commercial feasibility will heavily rely on delving more deeply into these aspects, along with the careful design of acceptor molecules to optimize desirable properties.

ACKNOWLEDGMENTS

T.M.C. would like to acknowledge the support from EPSRC Project No. EP/N026411/1. H.I.G. would like to acknowledge support from the EPSRC (EP/N509577/1, EP/T517793/1).

AUTHOR DECLARATIONS

Conflict of Interest

The authors have no conflicts to disclose.

Author Contributions

W.L. and T.M.C. researched and wrote the initial manuscript, with supporting sections written by R.J.E.W., J.G., and J.M.B. H.G. and T.M.C. designed the figures. All contributed to editing and finalizing the manuscript.

William Lowrie: Conceptualization (equal); Writing – original draft (equal). **Robert J. E. Westbrook:** Writing – original draft (equal); Writing – review & editing (equal). **Junjun Guo:** Writing – original draft (supporting); Writing – review & editing (supporting). **Hristo Gonev:** Visualization (equal); Writing – original draft (supporting); Writing – review & editing (supporting). **Jose Marin Beloqui:** Writing – original draft (equal); Writing – review & editing (supporting). **Tracey M. Clarke:** Conceptualization (lead); Project administration (lead); Supervision (lead); Visualization (lead); Writing – original draft (lead); Writing – review & editing (lead).

DATA AVAILABILITY

The data that support the findings of this study are available within the article and the references herein.

REFERENCES

- W. Zhao, S. Li, H. Yao, S. Zhang, Y. Zhang, B. Yang, and J. Hou, *J. Am. Chem. Soc.* **139**, 7148–7151 (2017).
- L. Zhu, M. Zhang, J. Xu, C. Li, J. Yan, G. Zhou, W. Zhong, T. Hao, J. Song, X. Xue, Z. Zhou, R. Zeng, H. Zhu, C.-C. Chen, R. C. I. MacKenzie, Y. Zou, J. Nelson, Y. Zhang, Y. Sun, and F. Liu, *Nat. Mater.* **21**, 656–663 (2022).
- A. Armin, W. Li, O. J. Sandberg, Z. Xiao, L. Ding, J. Nelson, D. Neher, K. Vandewal, S. Shoaee, T. Wang, H. Ade, T. Heumüller, C. Brabec, and P. Meredith, *Adv. Energy Mater.* **11**, 2003570 (2021).

- ⁴G. Zhang, F. R. Lin, F. Qi, T. Heumüller, A. Distler, H.-J. Egelhaaf, N. Li, P. C. Y. Chow, C. J. Brabec, A. K.-Y. Jen, and H.-L. Yip, *Chem. Rev.* **122**, 14180–14274 (2022).
- ⁵C. Yan, S. Barlow, Z. Wang, H. Yan, A. K.-Y. Jen, S. R. Marder, and X. Zhan, *Nat. Rev. Mater.* **3**, 18003 (2018).
- ⁶G. Zhang, J. Zhao, P. C. Y. Chow, K. Jiang, J. Zhang, Z. Zhu, J. Zhang, F. Huang, and H. Yan, *Chem. Rev.* **118**, 3447–3507 (2018).
- ⁷R. S. Gurney, D. G. Lidzey, and T. Wang, *Rep. Prog. Phys.* **82**, 036601 (2019).
- ⁸J. Hou, O. Inganäs, R. H. Friend, and F. Gao, *Nat. Mater.* **17**, 119–128 (2018).
- ⁹H. Ohkita, S. Cook, Y. Astuti, W. Duffy, S. Tierney, W. Zhang, M. Heeney, I. McCulloch, J. Nelson, D. D. C. Bradley, and J. R. Durrant, *J. Am. Chem. Soc.* **130**, 3030–3042 (2008).
- ¹⁰P. A. Lane, P. D. Cunningham, J. S. Melinger, O. Esenturk, and E. J. Heilweil, *Nat. Commun.* **6**, 7558 (2015).
- ¹¹H. Tamura and I. Burghardt, *J. Am. Chem. Soc.* **135**, 16364–16367 (2013).
- ¹²A. C. Jakowetz, M. L. Böhm, J. Zhang, A. Sadhanala, S. Huettner, A. A. Bakulin, A. Rao, and R. H. Friend, *J. Am. Chem. Soc.* **138**, 11672–11679 (2016).
- ¹³A. A. Bakulin, A. Rao, V. G. Pavelyev, P. H. M. van Loosdrecht, M. S. Pshenichnikov, D. Niedzialek, J. Cornil, D. Beljonne, and R. H. Friend, *Science* **335**, 1340–1344 (2012).
- ¹⁴A. C. Jakowetz, M. L. Böhm, A. Sadhanala, S. Huettner, A. Rao, and R. H. Friend, *Nat. Mater.* **16**, 551–557 (2017).
- ¹⁵K. Vandewal, S. Albrecht, E. T. Hoke, K. R. Graham, J. Widmer, J. D. Douglas, M. Schubert, W. R. Mateker, J. T. Bloking, G. F. Burkhard, A. Sellinger, J. M. J. Fréchet, A. Amassian, M. K. Riede, M. D. McGehee, D. Neher, and A. Salleo, *Nat. Mater.* **13**, 63–68 (2014).
- ¹⁶A. Y. Sosorev, D. Y. Godovsky, and D. Y. Paraschuk, *Phys. Chem. Chem. Phys.* **20**, 3658–3671 (2018).
- ¹⁷K. Kawashima, Y. Tamai, H. Ohkita, I. Osaka, and K. Takimiya, *Nat. Commun.* **6**, 10085 (2015).
- ¹⁸J. Liu, S. Chen, D. Qian, B. Gautam, G. Yang, J. Zhao, J. Bergqvist, F. Zhang, W. Ma, H. Ade, O. Inganäs, K. Gundogdu, F. Gao, and H. Yan, *Nat. Energy* **1**, 16089 (2016).
- ¹⁹M. C. Scharber, D. Mühlbacher, M. Koppe, P. Denk, C. Waldauf, A. J. Heeger, and C. J. Brabec, *Adv. Mater.* **18**, 789–794 (2006).
- ²⁰Y. Kim, S. A. Choulis, J. Nelson, D. D. C. Bradley, S. Cook, and J. R. Durrant, *J. Mater. Sci.* **40**, 1371–1376 (2005).
- ²¹L. M. Andersson and O. Inganäs, *Appl. Phys. Lett.* **88**, 082103 (2006).
- ²²K. Kanai, K. Akaike, K. Koyasu, K. Sakai, T. Nishi, Y. Kamizuru, T. Nishi, Y. Ouchi, and K. Seki, *Appl. Phys. A* **95**, 309–313 (2009).
- ²³C. M. Cardona, W. Li, A. E. Kaifer, D. Stockdale, and G. C. Bazan, *Adv. Mater.* **23**, 2367–2371 (2011).
- ²⁴T. M. Clarke, A. M. Ballantyne, J. Nelson, D. D. C. Bradley, and J. R. Durrant, *Adv. Funct. Mater.* **18**, 4029–4035 (2008).
- ²⁵Y. Zhong, M. Causa, G. J. Moore, P. Krauspe, B. Xiao, F. Günther, J. Kublitski, R. Shivhare, J. Benduhn, E. BarOr, S. Mukherjee, K. M. Yallum, J. Réhault, S. C. B. Mannsfeld, D. Neher, L. J. Richter, D. M. DeLongchamp, F. Ortman, K. Vandewal, E. Zhou, and N. Banerji, *Nat. Commun.* **11**, 833 (2020).
- ²⁶S. Karuthedath, J. Gorenflot, Y. Firdaus, N. Chaturvedi, C. S. P. De Castro, G. T. Harrison, J. I. Khan, A. Markina, A. H. Balawi, T. A. D. Peña, W. Liu, R.-Z. Liang, A. Sharma, S. H. K. Paleti, W. Zhang, Y. Lin, E. Alarousu, S. Lopatin, D. H. Anjum, P. M. Beaujuge, S. De Wolf, I. McCulloch, T. D. Anthopoulos, D. Baran, D. Andrienko, and F. Laquai, *Nat. Mater.* **20**, 378–384 (2021).
- ²⁷S.-i. Natsuda, T. Saito, R. Shirouchi, Y. Sakamoto, T. Takeyama, Y. Tamai, and H. Ohkita, *Energy Environ. Sci.* **15**, 1545–1555 (2022).
- ²⁸J. M. Hodgkiss, *Nat. Mater.* **20**, 289–290 (2021).
- ²⁹L. Perdígón-Toro, H. Zhang, A. Markina, J. Yuan, S. M. Hosseini, C. M. Wolff, G. Zuo, M. Stollerfoht, Y. Zou, F. Gao, D. Andrienko, S. Shoaee, and D. Neher, *Adv. Mater.* **32**, 1906763 (2020).
- ³⁰D. Qian, Z. Zheng, H. Yao, W. Tress, T. R. Hopper, S. Chen, S. Li, J. Liu, S. Chen, J. Zhang, X.-K. Liu, B. Gao, L. Ouyang, Y. Jin, G. Pozina, I. A. Buyanova, W. M. Chen, O. Inganäs, V. Coropceanu, J.-L. Bredas, H. Yan, J. Hou, F. Zhang, A. A. Bakulin, and F. Gao, *Nat. Mater.* **17**, 703–709 (2018).
- ³¹F. D. Eisner, M. Azzouzi, Z. Fei, X. Hou, T. D. Anthopoulos, T. J. S. Dennis, M. Heeney, and J. Nelson, *J. Am. Chem. Soc.* **141**, 6362–6374 (2019).
- ³²T. F. Hinrichsen, C. C. S. Chan, C. Ma, D. Paleček, A. Gillett, S. Chen, X. Zou, G. Zhang, H.-L. Yip, K. S. Wong, R. H. Friend, H. Yan, A. Rao, and P. C. Y. Chow, *Nat. Commun.* **11**, 5617 (2020).
- ³³A. Classen, C. L. Chochos, L. Lüer, V. G. Gregoriou, J. Wortmann, A. Osvet, K. Forberich, I. McCulloch, T. Heumüller, and C. J. Brabec, *Nat. Energy* **5**, 711–719 (2020).
- ³⁴M. S. Vezie, M. Azzouzi, A. M. Telford, T. R. Hopper, A. B. Sieval, J. C. Hummelen, K. Fallon, H. Bronstein, T. Kirchartz, A. A. Bakulin, T. M. Clarke, and J. Nelson, *ACS Energy Lett.* **4**, 2096–2103 (2019).
- ³⁵R. Englman and J. Jortner, *Mol. Phys.* **18**, 145–164 (1970).
- ³⁶E. Collado-Fregoso, S. N. Pugliese, M. Wojcik, J. Benduhn, E. Bar-Or, L. Perdígón Toro, U. Hörmann, D. Spoltore, K. Vandewal, J. M. Hodgkiss, and D. Neher, *J. Am. Chem. Soc.* **141**, 2329–2341 (2019).
- ³⁷X.-K. Chen, D. Qian, Y. Wang, T. Kirchartz, W. Tress, H. Yao, J. Yuan, M. Hülsbeck, M. Zhang, Y. Zou, Y. Sun, Y. Li, J. Hou, O. Inganäs, V. Coropceanu, J.-L. Bredas, and F. Gao, *Nat. Energy* **6**, 799–806 (2021).
- ³⁸W. Liu, S. Sun, L. Zhou, Y. Cui, W. Zhang, J. Hou, F. Liu, S. Xu, and X. Zhu, *Angew. Chem., Int. Ed.* **61**, e202116111 (2022).
- ³⁹Y. Liu, Z. Zheng, V. Coropceanu, J.-L. Brédas, and D. S. Ginger, *Mater. Horiz.* **9**, 325–333 (2022).
- ⁴⁰M. Azzouzi, N. P. Gallop, F. Eisner, J. Yan, X. Zheng, H. Cha, Q. He, Z. Fei, M. Heeney, A. A. Bakulin, and J. Nelson, *Energy Environ. Sci.* **15**, 1256 (2022).
- ⁴¹A. Köhler and H. Bässler, *Mater. Sci. Eng., R* **66**, 71–109 (2009).
- ⁴²S. M. Menke and R. J. Holmes, *Energy Environ. Sci.* **7**, 499–512 (2014).
- ⁴³S. D. Dimitrov, S. Wheeler, D. Niedzialek, B. C. Schroeder, H. Utzat, J. M. Frost, J. Yao, A. Gillett, P. S. Tuladhar, I. McCulloch, J. Nelson, and J. R. Durrant, *Nat. Commun.* **6**, 6501 (2015).
- ⁴⁴A. J. Gillett, A. Privitera, R. Dilmurat, A. Karki, D. Qian, A. Pershin, G. Londi, W. K. Myers, J. Lee, J. Yuan, S.-J. Ko, M. K. Riede, F. Gao, G. C. Bazan, A. Rao, T.-Q. Nguyen, D. Beljonne, and R. H. Friend, *Nature* **597**, 666–671 (2021).
- ⁴⁵S. Cook, H. Ohkita, J. R. Durrant, Y. Kim, J. J. Benson-Smith, J. Nelson, and D. D. C. Bradley, *Appl. Phys. Lett.* **89**, 101128 (2006).
- ⁴⁶J. J. Benson-Smith, H. Ohkita, S. Cook, J. R. Durrant, D. D. C. Bradley, and J. Nelson, *Dalton Trans.* **2009**, 10000–10005.
- ⁴⁷A. Privitera, J. Grüne, A. Karki, W. K. Myers, V. Dyakonov, T. Q. Nguyen, M. K. Riede, R. H. Friend, A. Sperlich, and A. J. Gillett, *Adv. Energy Mater.* **12**, 2103944 (2022).
- ⁴⁸A. Rao, P. C. Y. Chow, S. Gélinas, C. W. Schlenker, C.-Z. Li, H.-L. Yip, A. K.-Y. Jen, D. S. Ginger, and R. H. Friend, *Nature* **500**, 435–439 (2013).
- ⁴⁹P. C. Y. Chow, S. Gélinas, A. Rao, and R. H. Friend, *J. Am. Chem. Soc.* **136**, 3424–3429 (2014).
- ⁵⁰Z. Chen, X. Chen, Z. Jia, G. Zhou, J. Xu, Y. Wu, X. Xia, X. Li, X. Zhang, C. Deng, Y. Zhang, X. Lu, W. Liu, C. Zhang, Y. Yang, and H. Zhu, *Joule* **5**, 1832–1844 (2021).
- ⁵¹R. Wang, J. Xu, L. Fu, C. Zhang, Q. Li, J. Yao, X. Li, C. Sun, Z.-G. Zhang, X. Wang, Y. Li, J. Ma, and M. Xiao, *J. Am. Chem. Soc.* **143**, 4359–4366 (2021).
- ⁵²M. Shao, L. Yan, M. Li, I. Ilia, and B. Hu, *J. Mater. Chem. C* **1**, 1330–1336 (2013).
- ⁵³J. M. Marin-Belouqui, D. T. W. Toolan, N. A. Panjwani, S. Limbu, J.-S. Kim, and T. M. Clarke, *Adv. Energy Mater.* **11**, 2100539 (2021).
- ⁵⁴P. S. Maharjan and H. K. Bhattarai, *J. Oncol.* **2022**, 7211485.
- ⁵⁵Y. W. Soon, S. Shoaee, R. S. Ashraf, H. Bronstein, B. C. Schroeder, W. Zhang, Z. Fei, M. Heeney, I. McCulloch, and J. R. Durrant, *Adv. Funct. Mater.* **24**, 1474–1482 (2014).
- ⁵⁶Y. W. Soon, H. Cho, J. Low, H. Bronstein, I. McCulloch, and J. R. Durrant, *Chem. Commun.* **49**, 1291–1293 (2013).
- ⁵⁷A. M. Rao, P. Zhou, K.-A. Wang, G. T. Hager, J. M. Holden, Y. Wang, W.-T. Lee, X.-X. Bi, P. C. Eklund, D. S. Cornett, M. A. Duncan, and I. J. Amster, *Science* **259**, 955–957 (1993).
- ⁵⁸I. Ramirez, A. Privitera, S. Karuthedath, A. Jungbluth, J. Benduhn, A. Sperlich, D. Spoltore, K. Vandewal, F. Laquai, and M. Riede, *Nat. Commun.* **12**, 471 (2021).
- ⁵⁹A. Distler, T. Sauermann, H.-J. Egelhaaf, S. Rodman, D. Waller, K.-S. Cheon, M. Lee, and D. M. Guldi, *Adv. Energy Mater.* **4**, 1300693 (2014).
- ⁶⁰H. Zhang, A. Borgschulte, F. A. Castro, R. Crockett, A. C. Gerecke, O. Deniz, J. Heier, S. Jenatsch, F. Nüesch, C. Sanchez-Sanchez, A. Zoladek-Lemanczyk, and R. Hany, *Adv. Energy Mater.* **5**, 1400734 (2015).

- ⁶¹Q. Burlingame, X. Tong, J. Hankett, M. Sloatsky, Z. Chen, and S. R. Forrest, *Energy Environ. Sci.* **8**, 1005–1010 (2015).
- ⁶²Y. Che, M. R. Niazi, R. Izquierdo, and D. F. Perepichka, *Angew. Chem., Int. Ed.* **60**, 24833–24837 (2021).
- ⁶³J. Luke, E. J. Yang, Y. C. Chin, Y. Che, L. Winkler, D. Whatling, C. Labanti, S. Y. Park, and J. S. Kim, *Adv. Energy Mater.* **12**, 2201267 (2022).
- ⁶⁴P. E. Hartnett, E. A. Margulies, C. M. Mauck, S. A. Miller, Y. Wu, Y.-L. Wu, T. J. Marks, and M. R. Wasielewski, *J. Phys. Chem. B* **120**, 1357–1366 (2016).
- ⁶⁵Y. Kasai, Y. Tamai, H. Ohkita, H. Benten, and S. Ito, *J. Am. Chem. Soc.* **137**, 15980–15983 (2015).
- ⁶⁶H. L. Stern, A. Cheminal, S. R. Yost, K. Broch, S. L. Bayliss, K. Chen, M. Tabachnyk, K. Thorley, N. Greenham, J. M. Hodgkiss, J. Anthony, M. Head-Gordon, A. J. Musser, A. Rao, and R. H. Friend, *Nat. Chem.* **9**, 1205 (2017).
- ⁶⁷C. Simpson, T. M. Clarke, R. W. MacQueen, Y. Y. Cheng, A. J. Trevitt, A. J. Mozer, P. Wagner, T. W. Schmidt, and A. Nattestad, *Phys. Chem. Chem. Phys.* **17**, 24826–24830 (2015).
- ⁶⁸T. Dilbeck and K. Hanson, *J. Phys. Chem. Lett.* **9**, 5810–5821 (2018).
- ⁶⁹J. Guo, B. Moss, and T. M. Clarke, *J. Mater. Chem. A* **10**, 20874–20885 (2022).
- ⁷⁰F. Kraffert, R. Steyrluehner, C. Meier, R. Bittl, and J. Behrends, *Appl. Phys. Lett.* **107**, 043302 (2015).
- ⁷¹Y. Wang and X. Zhan, *Adv. Energy Mater.* **6**, 1600414 (2016).
- ⁷²C.-F. Lin, V. M. Nichols, Y.-C. Cheng, C. J. Bardeen, M.-K. Wei, S.-W. Liu, C.-C. Lee, W.-C. Su, T.-L. Chiu, H.-C. Han, L.-C. Chen, C.-T. Chen, and J.-H. Lee, *Sol. Energy Mater. Sol. Cells* **122**, 264–270 (2014).
- ⁷³S. Y. Leblebici, L. Catane, D. E. Barclay, T. Olson, T. L. Chen, and B. Ma, *ACS Appl. Mater. Interfaces* **3**, 4469–4474 (2011).
- ⁷⁴A. Markina, K. H. Lin, W. Liu, C. Poelking, Y. Firdaus, D. R. Villalva, J. I. Khan, S. H. K. Paleti, G. T. Harrison, J. Gorenflot, W. Zhang, S. De Wolf, I. McCulloch, T. D. Anthopoulos, D. Baran, F. Laquai, and D. Andrienko, *Adv. Energy Mater.* **11**, 2102363 (2021).
- ⁷⁵R. Sun, J. Guo, Q. Wu, Z. Zhang, W. Yang, J. Guo, M. Shi, Y. Zhang, S. Kahmann, L. Ye, X. Jiao, M. A. Loi, Q. Shen, H. Ade, W. Tang, C. J. Brabec, and J. Min, *Energy Environ. Sci.* **12**, 3118–3132 (2019).
- ⁷⁶Q. He, W. Sheng, M. Zhang, G. Xu, P. Zhu, H. Zhang, Z. Yao, F. Gao, F. Liu, X. Liao, and Y. Chen, *Adv. Energy Mater.* **11**, 2003390 (2021).
- ⁷⁷J. Zhang, M. H. Futscher, Y. Lami, F. U. Kosasih, C. Cho, Q. Gu, A. Sadhanala, A. J. Pearson, B. Kan, G. Divitini, X. Wan, D. Credgington, N. C. Greenham, Y. Chen, C. Ducati, B. Ehrler, Y. Vaynzof, R. H. Friend, and A. A. Bakulin, *Adv. Energy Mater.* **9**, 1902145 (2019).
- ⁷⁸Y. Li and Y. Lin, *J. Mater. Chem. C* **9**, 11715–11721 (2021).
- ⁷⁹K. Jiang, J. Zhang, Z. Peng, F. Lin, S. Wu, Z. Li, Y. Chen, H. Yan, H. Ade, Z. Zhu, and A. K.-Y. Jen, *Nat. Commun.* **12**, 468 (2021).
- ⁸⁰J. Wan, L. Zeng, X. Liao, Z. Chen, S. Liu, P. Zhu, H. Zhu, and Y. Chen, *Adv. Funct. Mater.* **32**, 2107567 (2022).
- ⁸¹K. Jiang, J. Zhang, C. Zhong, F. R. Lin, F. Qi, Q. Li, Z. Peng, W. Kaminsky, S.-H. Jang, J. Yu, X. Deng, H. Hu, D. Shen, F. Gao, H. Ade, M. Xiao, C. Zhang, and A. K.-Y. Jen, *Nat. Energy* **7**, 1076–1086 (2022).
- ⁸²W. Gao, F. Qi, Z. Peng, F. R. Lin, K. Jiang, C. Zhong, W. Kaminsky, Z. Guan, C. S. Lee, T. J. Marks, H. Ade, and A. K. Y. Jen, *Adv. Mater.* **34**, 2202089 (2022).
- ⁸³L. Huang, P. Jiang, Y. Zhang, L. Zhang, Z. Yu, Q. He, W. Zhou, L. Tan, and Y. Chen, *ACS Appl. Mater. Interfaces* **11**, 26213–26221 (2019).
- ⁸⁴D. Zhang, W. Zhong, L. Ying, B. Fan, M. Li, Z. Gan, Z. Zeng, D. Chen, N. Li, F. Huang, and Y. Cao, *Nano Energy* **85**, 105957 (2021).
- ⁸⁵Y. Yan, X. Zhou, F. Zhang, J. Zhou, T. Lin, Y. Zhu, D. Xu, X. Ma, Y. Zou, and X. Li, *J. Mater. Chem. A* **10**, 23124–23133 (2022).
- ⁸⁶X. Wang, L. Zhang, L. Hu, Z. Xie, H. Mao, L. Tan, Y. Zhang, and Y. Chen, *Adv. Funct. Mater.* **31**, 2102291 (2021).
- ⁸⁷X. Zhang, Y. Li, D. Zhang, G. Wu, H. Zhang, J. Zhou, X. Li, Z. Saud-uz-Zafar, J. Zhang, Z. Wei, H. Zhou, and Y. Zhang, *Sci. China: Chem.* **64**, 116–126 (2021).
- ⁸⁸Y. Song, K. Zhang, S. Dong, R. Xia, F. Huang, and Y. Cao, *ACS Appl. Mater. Interfaces* **12**, 18473–18481 (2020).
- ⁸⁹S. Dong, K. Zhang, B. Xie, J. Xiao, H.-L. Yip, H. Yan, F. Huang, and Y. Cao, *Adv. Energy Mater.* **9**, 1802832 (2019).
- ⁹⁰S. Liu, D. Chen, X. Hu, Z. Xing, J. Wan, L. Zhang, L. Tan, W. Zhou, and Y. Chen, *Adv. Funct. Mater.* **30**, 2003223 (2020).
- ⁹¹L. Zhang, H. Zhao, J. Yuan, B. Lin, Z. Xing, X. Meng, L. Ke, X. Hu, W. Ma, and Y. Yuan, *Org. Electron.* **83**, 105771 (2020).
- ⁹²Y. Cai, Q. Li, G. Lu, H. S. Ryu, Y. Li, H. Jin, Z. Chen, Z. Tang, G. Lu, X. Hao, H. Y. Woo, C. Zhang, and Y. Sun, *Nat. Commun.* **13**, 2369 (2022).
- ⁹³R. Wang, Y. Jiang, W. Gruber, Y. He, M. Wu, P. Weitz, K. Zhang, L. Luer, K. Forberich, T. Unruh, E. Spiecker, C. Deibel, N. Li, and C. J. Brabec, *Adv. Mater. Interfaces* **9**, 2200342 (2022).
- ⁹⁴S. M. Menke, A. Cheminal, P. Conaghan, N. A. Ran, N. C. Greehnam, G. C. Bazan, T.-Q. Nguyen, A. Rao, and R. H. Friend, *Nat. Commun.* **9**, 277 (2018).
- ⁹⁵N. A. Ran, S. Roland, J. A. Love, V. Savikhin, C. J. Takacs, Y.-T. Fu, H. Li, V. Coropceanu, X. Liu, J.-L. Brédas, G. C. Bazan, M. F. Toney, D. Neher, and T.-Q. Nguyen, *Nat. Commun.* **8**, 79 (2017).
- ⁹⁶S. Y. Park, S. Chandrabose, M. B. Price, H. S. Ryu, T. H. Lee, Y. S. Shin, Z. Wu, W. Lee, K. Chen, S. Dai, J. Zhu, P. Xue, X. Zhan, H. Y. Woo, J. Y. Kim, and J. M. Hodgkiss, *Nano Energy* **84**, 105924 (2021).
- ⁹⁷S. R. Scully and M. D. McGehee, *J. Appl. Phys.* **100**, 034907 (2006).
- ⁹⁸W. A. Luhman and R. J. Holmes, *Adv. Funct. Mater.* **21**, 764–771 (2011).
- ⁹⁹X. Lai, H. Lai, M. Du, H. Chen, D. Qiu, Y. Zhu, M. Pu, Y. Zhu, E. Zhou, and F. He, *Chem. Mater.* **34**, 7886–7896 (2022).
- ¹⁰⁰Q. Yue, W. Liu, and X. Zhu, *J. Am. Chem. Soc.* **142**, 11613–11628 (2020).
- ¹⁰¹Q. Liu, Y. Jiang, K. Jin, J. Qin, J. Xu, W. Li, J. Xiong, J. Liu, Z. Xiao, K. Sun, S. Yang, X. Zhang, and L. Ding, *Sci. Bull.* **65**, 272–275 (2020).
- ¹⁰²A. Guerrero and G. Garcia-Belmonte, *Nano-Micro Lett.* **9**, 10 (2016).
- ¹⁰³H. B. Naveed and W. Ma, *Joule* **2**, 621–641 (2018).
- ¹⁰⁴D. Baran, R. S. Ashraf, D. A. Hanifi, M. Abdelsamie, N. Gasparini, J. A. Röhr, S. Holliday, A. Wadsworth, S. Lockett, M. Neophytou, C. J. M. Emmott, J. Nelson, C. J. Brabec, A. Amassian, A. Salleo, T. Kirchartz, J. R. Durrant, and I. McCulloch, *Nat. Mater.* **16**, 363–369 (2017).
- ¹⁰⁵J. Roncali and I. Grosu, *Adv. Sci.* **6**, 1801026 (2019).
- ¹⁰⁶I. G. Scheblykin, A. Yartsev, T. Pullerits, V. Gulbinas, and V. Sundström, *J. Phys. Chem. B* **111**, 6303–6321 (2007).
- ¹⁰⁷M. B. Price, P. A. Hume, A. Ilina, I. Wagner, R. R. Tamming, K. E. Thorn, W. Jiao, A. Goldingay, P. J. Conaghan, G. Lakhwani, N. J. L. K. Davis, Y. Wang, P. Xue, H. Lu, K. Chen, X. Zhan, and J. M. Hodgkiss, *Nat. Commun.* **13**, 2827 (2022).
- ¹⁰⁸H. Ohkita, S. Cook, Y. Astuti, W. Duffy, M. Heeney, S. Tierney, I. McCulloch, D. D. C. Bradley, and J. R. Durrant, *Chem. Commun.* **2006**, 3939.
- ¹⁰⁹G. Grancini, M. De Bastiani, N. Martino, D. Fazzi, H.-J. Egelhaaf, T. Sauer-mann, M. R. Antognazza, G. Lanzani, M. Caironi, L. Franco, and A. Petrozza, *Phys. Chem. Chem. Phys.* **16**, 8294–8300 (2014).
- ¹¹⁰Y. Dong, V. C. Nikolis, F. Talmack, Y.-C. Chin, J. Benduhn, G. Londi, J. Kublitski, X. Zheng, S. C. B. Mannsfeld, D. Spoltore, L. Muccioli, J. Li, X. Blase, D. Beljonne, J.-S. Kim, A. A. Bakulin, G. D’Avino, J. R. Durrant, and K. Vandewal, *Nat. Commun.* **11**, 4617 (2020).
- ¹¹¹N. V. Hoang, V. C. Nikolis, L. Baisinger, K. Vandewal, and M. S. Pshenichnikov, *Phys. Chem. Chem. Phys.* **23**, 20848–20853 (2021).
- ¹¹²S. Li, X. Yuan, Q. Zhang, B. Li, Y. Li, J. Sun, Y. Feng, X. Zhang, Z. Wu, H. Wei, M. Wang, Y. Hu, Y. Zhang, H. Y. Woo, J. Yuan, and W. Ma, *Adv. Mater.* **33**, 2101295 (2021).
- ¹¹³Y. Wu, J. Guo, W. Wang, Z. Chen, Z. Chen, R. Sun, Q. Wu, T. Wang, X. Hao, H. Zhu, and J. Min, *Joule* **5**, 1800–1815 (2021).
- ¹¹⁴X. Jiang, J. Yang, S. Karuthedath, J. Li, W. Lai, C. Li, C. Xiao, L. Ye, Z. Ma, Z. Tang, F. Laquai, and W. Li, *Angew. Chem., Int. Ed.* **59**, 21683–21692 (2020).